POLITECNICO MILANO 1863

SCUOLA DI INGEGNERIA INDUSTRIALE E DELL'INFORMAZIONE

EXECUTIVE SUMMARY OF THE THESIS

Inclusion of the pre-stress in patient-specific models of aortas for TAVI procedure simulations

MASTER THESIS IN BIOMEDICAL ENGINEERING

AUTHOR: MATTIA FARINA, GIULIA MORA

ADVISOR: Prof. JOSE FELIX RODRIGUEZ MATAS

CO-ADVISOR: Dott. Ing. GIULIA LURAGHI

ACADEMIC YEAR: 2021-2022

1. Introduction

The evolution of medicine, in the cardiovascular field especially, is moving towards the development of patient-specific surgery solutions. The patient-specific computational models, used in pre-operative planning, are generated starting from diagnostic images, in which the vascular tissue is in a pre-deformed state as subjected to blood pressure (Figure 1). However, most of the models in the literature consider stress-free the geometry reconstructed from images, which leads to the total loss of information related to pre-deformation and residual stresses within the tissue.

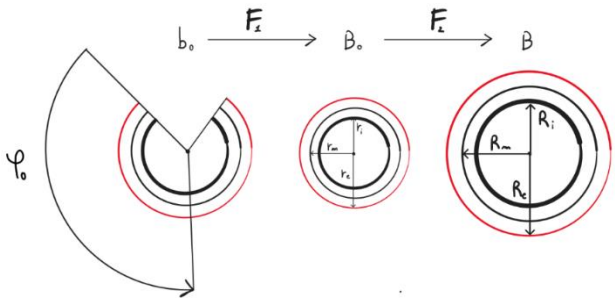

Figure 1. Different configurations of the aorta: opened section (b_0), undeformed (B_0) and pressurized (B) configurations.

This work continues the *ZeroPressure* algorithm developed by Fantaci and Franceschelli [1] which implements, among the different methods for obtaining the zero-pressure configuration, the inverse elastostatics method with exact linearization. The algorithm is modified with the aim of making it applicable to complex patient-specific aorta computational models. These can be used in finite element structural simulations of clinical procedures, such as TAVI (Transcatheter Aortic Valve Implantation) intervention.

The TAVI procedure is a treatment for patients suffering from acute aortic stenosis (AS) and who are unsuitable for surgery, because they are considered patients at risk. This methodology, in fact, allows the implantation of an aortic valve (consisting of biological leaflets and skirt) mounted on a stent, without the need for open heart surgery. Procedural safety can be improved by following an engineering approach. The combination of high-resolution imaging and finite element analysis techniques makes it possible to virtually implant transcatheter valves and understand the interaction of the device with its complex anatomical surroundings.

There has been a considerable evolution of TAVI simulations, but none of these include the pre-stress in the initial geometry of the virtual model. If this additional information was included, the outcomes of the simulations might bring the prediction closer to the real case, improving its reliability and therefore the safety of the clinical procedures based on them.
This work has a twofold goal: firstly, to modify the algorithm with the aim to obtain the zero-pressure configuration of two patient-specific aortas and subsequently to verify whether the inclusion of the stresses, deriving from the pre-stressed condition, in the virtual models of the aortas might be significant for the outcome of TAVI procedure simulations.

2. Materials and Methods

In the work, two patient-specific aortic roots obtained by TAC segmentation are used, named PatientA and PatientB. The native valve is not considered in the first section of the work and will be introduced afterwards. The pre-processing phase is implemented in ANSA Pre-Processor v22.0.1 (BETA CAE Systems, Switzerland). After the removal of superficial and internal artifacts, each aortic root is meshed with triangular shell elements with a dimension of 0.8 mm and, for the coronaries, 0.5 mm; onto this superficial mesh, a three layers 3D tetra-mesh is built with a thickness of 2.1 mm for the aorta and 0.7 mm for the coronaries, with a transition region between these two with a 1.4 mm thickness. The internal pressure p is set at 80 mmHg (0.0107 MPa), corresponding to the pressure at which the TAC images were obtained. Node sets are defined on the inlet and outlets (of the aorta and the coronaries) and constrained in all the directions. Moreover, an element-set is identified following the valve-sinuses attachments (named sinuses profile) in order to define a material that is different to the one of the aortic wall. The reason behind this choice lies in the particular shape of this region, characterized by concave areas that would collapse (collision between two opposite sides of the aortic wall) and make the algorithm diverge.
Since the *ZeroPressure* algorithm works with the Abaqus syntax, at the end of the pre-processing phase the Abaqus input file is obtained.

2.1. ZeroPressure algorithm

Input function
The input function is aimed to rearrange the information contained in the Abaqus input file in a proper way to be read by the algorithm. More precisely, it organizes data in vectors and matrices with a proper structure. This function also assigns the material properties to the aortic wall and the element-set previously defined.

ZeroPressure algorithm
The *ZeroPressure* algorithm [1] is the main subject of the procedure. Starting from a deformed geometry with properly defined boundary conditions and knowing the load that has caused that deformation, this algorithm performs the inverse finite elastostatic method, giving back the undeformed configuration of the geometry: applying this to the patient-specific aorta, the vessel configuration without blood pressure action can be found. Some adjustments are done to the original algorithm to let it work with different materials and sets: in our case, only two materials are needed but, following the modifications, including more information and parts is a straightforward procedure.
To calculate the undeformed configuration, the applied pressure p is divided into a user-defined number of increments. Starting from $p = 0$, several iterative cycles are performed in order to minimize the residual $\boldsymbol{res}$ between the external force $\boldsymbol{fext}$, constant for the increment, and the internal one $\boldsymbol{fint}$, computed at each iteration:

$$\boldsymbol{res} = \boldsymbol{fext} - \boldsymbol{fint} \qquad (1.\ 1)$$

When the residual is under a defined value, the next pressure increment is added and the calculation starts again. The algorithm ends when it reaches the last increment, corresponding to the whole pressure load.
The principal equations on which this algorithm is based are here reported. They are all computed for a single element and then assembled. The external force for each element is defined as

$$\boldsymbol{f}_{ext}^{(e)} = pA_{face}\boldsymbol{n} \qquad (1.\ 2)$$

where $\mathbf{n}$ is the unit vector normal to the element face. The element internal force is calculated as

$$\boldsymbol{f}_{int}^{(e)} = \sum_{i=1}^{npg} \omega_i \widehat{\boldsymbol{B}}^T \cdot \boldsymbol{\sigma}\, J_i \qquad (1.\ 3)$$

where npg is the number of Gauss integration points, ω is the relative weight of the considered Gauss point, $\boldsymbol{B}$ is the matrix that contains the

	$C_{10}[MPa]$	$C_{20}[MPa]$	$C_{30}[MPa]$	ν	$D[MPa^{-1}]$
Aortic wall	0.0417	0.1186	0.4550	0.48	0.9725
Sinuses profile	0.4705	6.4110	0	0.48	0.0862

Table 1. Material properties set for the model; coefficients are the same for both the aortic wall and the coronaries.

derivatives of the shape functions, $J = \det(\boldsymbol{J})$ is the Jacobian and $\boldsymbol{\sigma}$ is the stress tensor calculated as

$$\boldsymbol{\sigma} = \frac{1}{J}\boldsymbol{F}_2\boldsymbol{S}\boldsymbol{F}_2^T \qquad (1.4)$$

in which $\boldsymbol{F}_2$ is the deformation gradient and $\boldsymbol{S} = 2\frac{\partial W}{\partial C}$ is the Second Piola-Kirchoff Stress Tensor. This is calculated starting from the energy function W, which depends on the material. The algorithm is built to be used with three different material models: generalized Yeoh, modified Holzapfel-Gasser-Ogden (HGO) and Nolan. Since the elastic response of the healthy human aorta seems to be independent from the applied load direction [2], the Yeoh model for hyperelastic materials was used:

$$W = C_{10}(\bar{I}_1 - 3) + C_{20}(\bar{I}_1 - 3)^2 + C_{30}(\bar{I}_1 - 3)^3 + \frac{1}{D}(J-1)^2 \qquad (1.5)$$

where C_{10}, C_{20} and C_{30} are material parameters. Due to the strong relationship between the geometry behavior and its thickness, these parameters are obtained fitting the stress-strain curves obtained by Azadani et al. [2] (for the aortic wall) and those obtained by Marom et al. [2] (for the sinuses profile) (Table 1).

Output Function

The results of the algorithm need to be written in a proper way, so that LS-Dyna R12 (ANSYS) can read them. In fact, this finite element solver is used to re-pressurize the geometry in order to get back the initial geometry, with the inclusion of the pre-stress state.

Pressurization

Once the zero-pressure configuration is computed, the pressurization simulation is set to obtain the inflated geometry with the pre-stress inclusion. To do so, a 0-1 ramp load in 100 ms and an internal pressure of 80 mmHg are imposed. As previously said, also in this case the extremities are fixed. A damping coefficient on the geometry is set to 0.001 ms^{-1}.

Geometries comparison

A Matlab script is written to make a comparison between the starting geometry and the one obtained after the application of the pressure load. The code contains the following equations used to calculate the normalized error RMS and the percentage error $ERR\%$:

$$RMS = \sqrt{\frac{\sum(N_{P_i} - N_{F_i})^2}{\sum(N_{F_i})^2}} \qquad (1.6)$$

$$ERR\% = 100\, RMS\,\% \qquad (1.7)$$

where N_{P_i} are the pre-stress configuration nodes and N_{F_i} are those of the starting geometry.

2.2. TAVI simulations

Model preparation

The aortas of the two patients are used for finite elements structural simulations to reproduce the TAVI procedure. The simulations are performed starting from the deformed configuration, considering or not the inclusion of the pre-stress for both the patients and evaluating differences in terms of stent positioning, vascular damage and atrioventricular block. The model parts are 23, treated as follows [4].

The aortic wall and sinuses profile geometries are the same as previously described. The addition of the aortic internal wall (shell layer) is necessary to set contacts between parts. To draw the native valve, the leaflet surfaces are generated by following reference points identified at the commissures and basal leaflet attachment lines on the aortic lumen. They are meshed with 4048 Belytschko–Lin–Tsay triangular shell elements. Calcium deposits are discretized using 9516 tetrahedral elements. Also in this case, the external surface made by triangular elements is added with the aim to set contacts. Both the native valve and calcium deposits are modelled as linear elastic materials (Table 3). The transcatheter valve used in this work is the CoreValve Evolute R (Medtronic, Minneapolis, MN, USA) made by three components: stent, skirt and leaflets. The stent,

	Description	*Value*
E^A	Austenite (A) elastic modulus	$5.170x10^4\ MPa$
E^M	Martensite (M) elastic modulus	$4.780x10^4\ MPa$
$\boldsymbol{\nu}$	Poisson's ratio	0.3
σ_L^S	Initial stress A→M transformation	$600\ MPa$
σ_L^E	End stress A→M transformation	$670\ MPa$
σ_U^S	Initial stress M→A transformation	$288\ MPa$
σ_U^E	End stress M→A transformation	$254\ MPa$
$\left(\frac{\partial\sigma}{\partial T}\right)_L$	Stress-temperature coefficient A→M transformation	$2.1\ MPa\ K^{-1}$
$\left(\frac{\partial\sigma}{\partial T}\right)_U$	Stress-temperature coefficient M→A transformation	$2.1\ MPa\ K^{-1}$
T_0	Reference temperature	$310\ K$
ε^L	Maximum transformation strain	6.3%
ε_V^L	Maximum volumetric transformation strain	6.3%

Table 2. Mechanical properties of shape-memory NiTi alloy.

which has a non-constant longitudinal diameter, is modelled with 5340 Hunghs-Liu beam elements. Its material properties are those of the shape-memory NiTi (Table 2). The leaflets are meshed with 3840 quadrilateral shell elements with hourglass viscosity control and full integration. They are modeled as hyperelastic materials (Table 4). There are 29538 triangular Belytschko-Tsay shell elements to discretize the skirt. Moreover, a selective mass scaling is introduced to keep the time step constant to 10^{-6} s.
Other important components are the two catheters, one for the device crimping and one for its release and twelve crimping rigid planes to move the device inside the catheter.

Simulations
The device positioning, crimping and release phases are considered in the simulations. The device is positioned so that the leaflets annulus lies on the same plane of the natural annulus, as suggested by the cardiac surgeon. Using the twelve rigid planes, the diameter of the device is uniformly crimped down to 0.9 mm into a rigid catheter; then, it is released in the second catheter which is slowly lifted towards the aortic arch to let the device open. Moreover, a 0.2 friction coefficient is set for stent-aortic internal wall, stent-native valve and stent-calcium deposits contacts. Also in this case, the aortic extremities are fixed.

	Native valve	*Calcium deposits*
$\rho\ [Kg/m^3]$	1100	2000
ν	0.40	0.45
$E\ [MPa]$	0.10	12.60

Table 3. Mechanical properties of the native valve and the calcium deposits.

	Leaflets
$\rho\ [Kg/m^3]$	1060
ν	0.49
$C_{10}\ [MPa]$	81.2814
$C_{01}\ [MPa]$	10^{-4}
$C_{11}\ [MPa]$	$6.22\ x10^5$

Table 4. Mechanical properties of the leaflets.

3. Results and Discussion

3.1. ZeroPressure algorithm

Zero-pressure configuration
The first results of the *ZeroPressure* algorithm are related to the choice of the material properties and the correct constraints that better reproduce the physiological behavior of the aortic wall, the sinuses profile and the coronaries. After several attempts regarding stiffer or softer materials, the parameters reported in Table 1 are chosen. Despite the good response of the material proposed by Azadani et al. [2], the geometry would collapse if the stiffer sinuses profile region was not added. Moreover, the decision to fix coronaries outlets is made to reproduce a more physiological condition, instead of fixing their roots
At the end, the zero-pressure configuration is successfully obtained for both the considered patients.

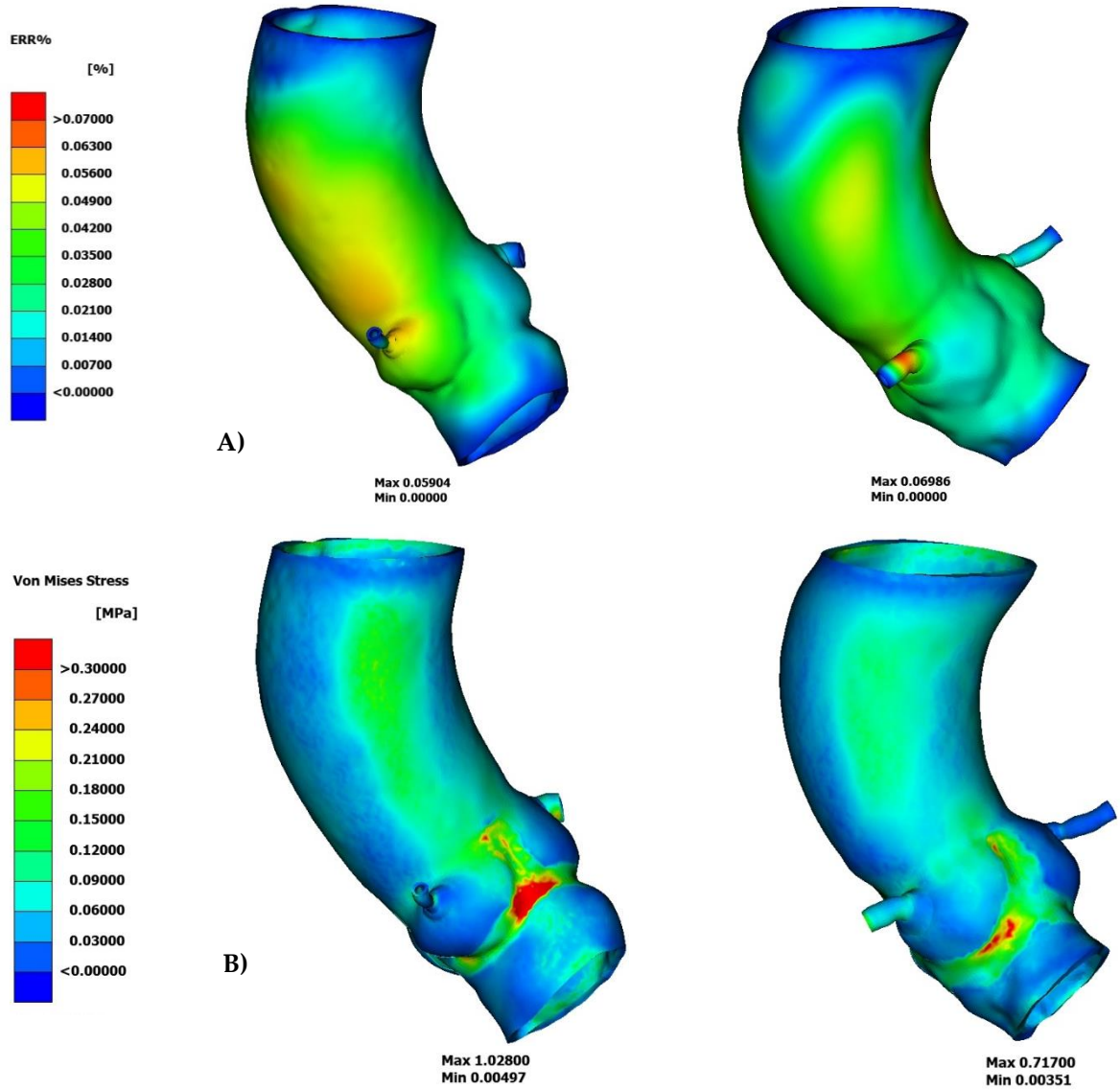

Figure 2. Distribution of percentage error (**A**) and Von Mises Stress (**B**) for PatientA (left) and PatientB (right).

Pre-stress inclusion

The pressure load is then applied to the obtained zero-pressure geometries. The main objective of this phase is to obtain a geometry that is entirely equivalent to the starting one (from imaging) but that contains the pre-stress state. Computing the error in (1. 6) and (1. 7), it is found that the two configurations are quite the same (Figure 2.A). In fact, the maximum percentage error is equal to 0.0590% for PatientA and 0.0699% for PatientB. The attention is focused on the fact that, using the input function to turn the Abaqus input file in a format readable by the algorithm, those digits after the fourth decimal place are lost, making the error even less relevant. Figure 2.B shows the stress distribution for PatientA and PatientB.

3.2. TAVI simulations

Results are reported in terms of device positioning, vascular damage and atrioventricular block.

Device positioning

This is evaluated considering the contact area, the aorta-stent distance and Von-Mises stresses on the stent.

In the configuration including the pre-stress state, the contact area is 5.0834% smaller for PatientA and 10.3406% higher for PatientB. Except for this opposite trend, results show small differences between the two configurations, in both the considered patients.

The aorta-stent distance should be equal to zero near the annulus to guarantee a good connection between the two parts. For both the patients,

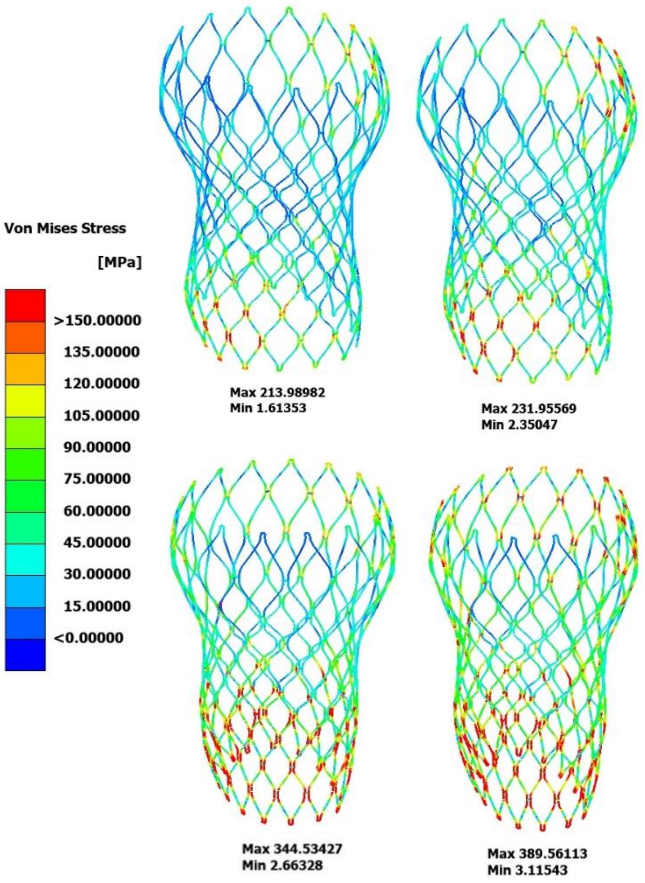

Figure 3. Distribution of Von Mises stresses on the stent for PatientA (top) and PatientB (bottom). For each patient, it is showed the final configuration of the stent in the unstressed (left) and pre-stressed (right) geometry.

results show a lower distance (that means a better adhesion of the device) in this region in the pre-stressed configuration; on the contrary, the distance increases leaving the annulus, both towards the aortic arch and the ventricle, for the same configuration.

Von-Mises stresses on the stent are useful to predict its failure due to fatigue. In addition to a smaller opening diameter reached after the expansion of the device, a completely different stress distribution is found in the pre-stressed configuration: not only higher values are reached but also an increased number of points is subjected to this amount of stress (Figure 3).

Hence, the pre-stress inclusion leads to the prediction of adhesion of the device that is better at the annuls region and worse in the distal zone if compared to the unstressed configuration. This is due to a lower deployed diameter of the stent. This also explains the change in the stress distribution: the inclusion of the pre-stress state leads to considerations about the positioning that differs from the unstressed case.

Vascular damage

The main feature used to quantify vascular damage is the stress distribution in the arterial wall. More precisely, First Principal stresses are considered (Figure 4). In fact, high concentrated stresses can determine damage of the aortic wall and the occurrence of fatal events. As one can expect, the inclusion of the pre-stress state in the geometry brings the wall stresses closer to a limit condition.

Atrioventricular block

The occurrence of the atrioventricular block is evaluated through the contact pressure between the stent and the aorta. The deformation of the aortic wall, due to the device, can determine the compression of the atrioventricular conduction

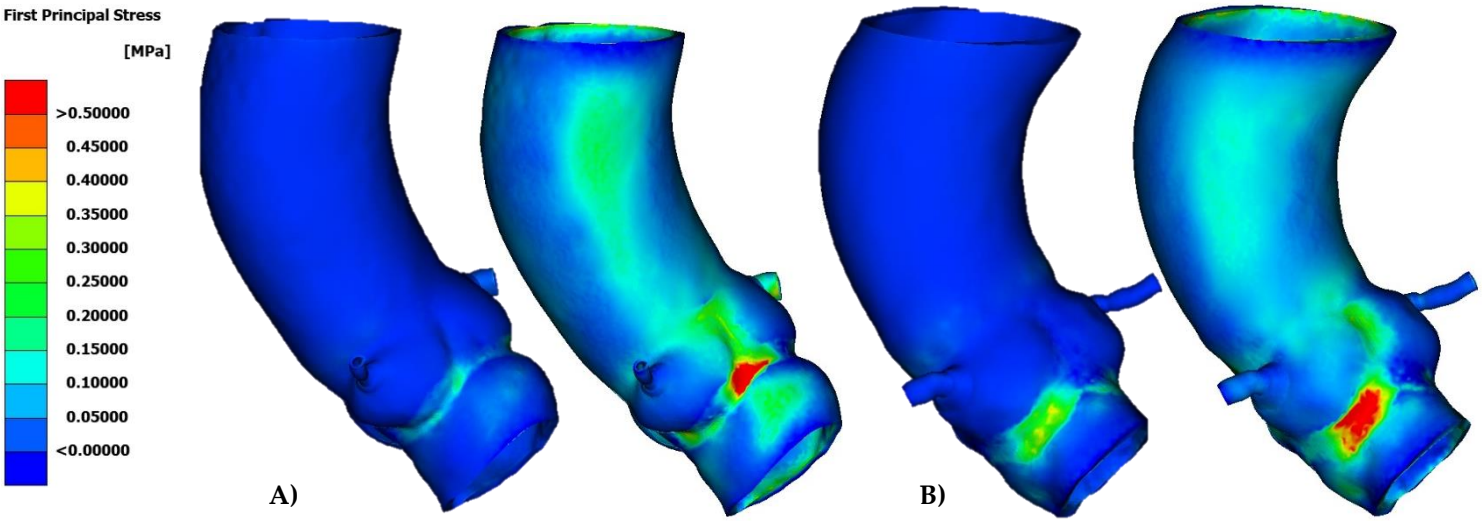

Figure 4. First Principal Stresses comparison between the two configurations in PatientA (**A**) and PatientB (**B**).

system, modifying the propagation of the electrical impulse and requiring the implantation of a permanent pacemaker (PPM).

Also in this case, for both patients, what changes between the two configurations is not so much the spatial distribution of the pressure as its local values. Although the maximum value is very similar in the two configurations, there is a greater presence of high contact pressure in the same areas (Figure 5).

In a recent retroactive study [5], First Principal Strains were evaluated on the portion of the aortic root between the non-coronary sinus and the right coronary sinus where the left bundle branch is located, because larger values of strain imply greater forces exerted by the expanded device to lengthen the implant site, and therefore the potential risk of conduction abnormalities. In the aforementioned study, the simulations resulted in a maximum strain value of 24.5% in the area of interest for a patient who required PPM implant, which differed greatly from the average of the

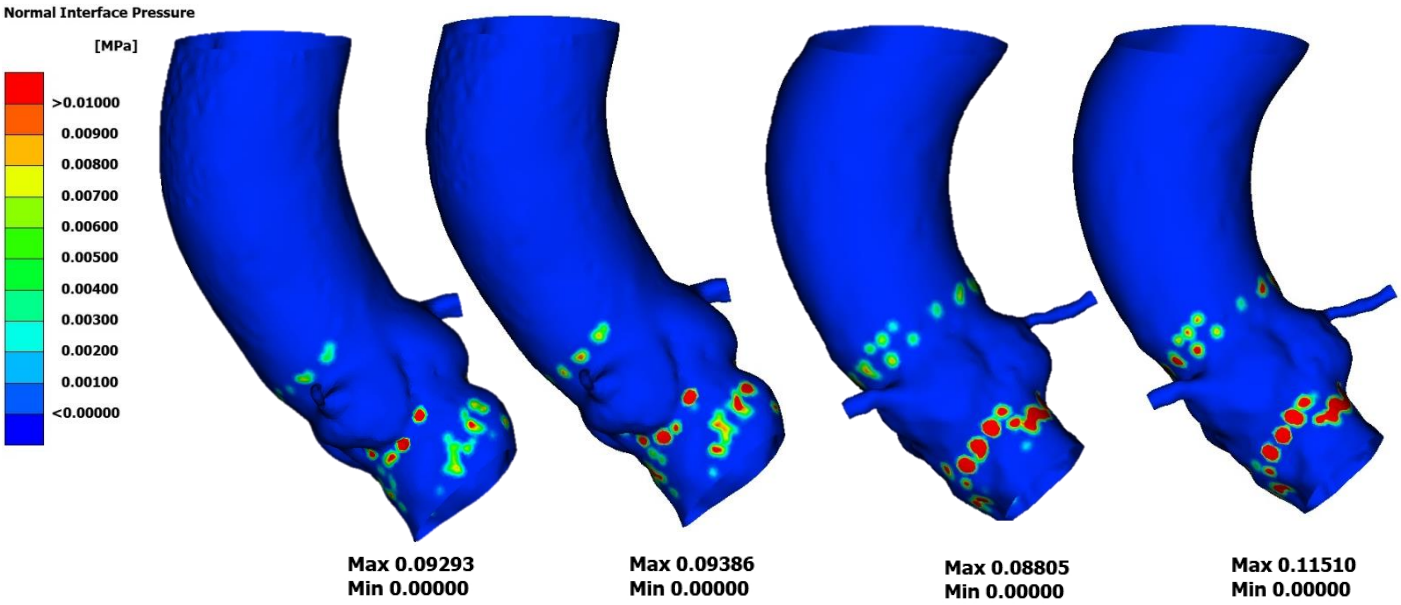

Figure 5. Contact pressure between the stent and the aorta in the unstressed and pre-stressed configuration for PatientA (**A**) and PatientB (**B**).

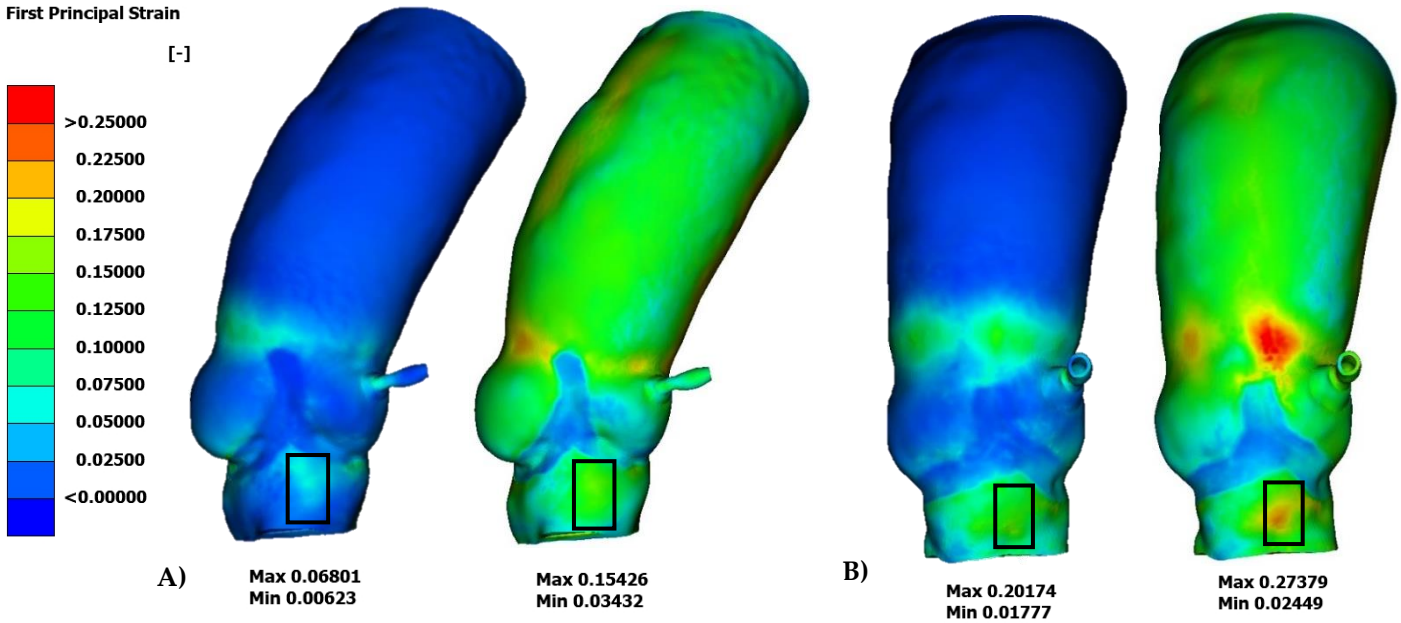

Figure 6. Distribution of First Principal Strain in the unstressed (left) and pre-stressed (right) configuration for PatientA (**A**) and PatientB (**B**). It is also showed the area in which conduction abnormalities are evaluated and reported maximum and minimum values related to this region.

maximum values of all the patients which is 13.8%, indicating a possible correlation between the strain in that specific area and the development of atrioventricular block. In this work, the maximum value of First Principal Strain obtained in the area of interest is 15.4% in the configuration including the pre-stress, compared to 6.8% in the configuration without the pre-stress in PatientA and 20.2% and 27.4% respectively in PatientB (Figure 6).

In both patients, the difference between the maximum strains resulting from the two configurations ($\varepsilon_{\text{pre-stress}} - \varepsilon_{\text{no pre-stress}} \sim 10\%$, with ε = First Principal Strain) is comparable to the difference between those in patients with and without PPM in Bosi et al. [5] ($\varepsilon_{\text{PPM}} - \varepsilon_{\text{no PPM}} \sim 10\%$). This shows how the absence of the pre-stress might lead to underestimating the effects of the implant, especially when the deformations are in a high range as for PatientB.

In both patients, the difference between the maximum strains resulting from the two configurations ($\varepsilon_{\text{pre-stress}} - \varepsilon_{\text{no pre-stress}} \sim 10\%$, with ε = First Principal Strain) is comparable to the difference between those in patients with and without PPM in Bosi et al. [5] ($\varepsilon_{\text{PPM}} - \varepsilon_{\text{no PPM}} \sim 10\%$). This shows how the absence of the pre-stress might lead to underestimating the effects of the implant, especially when the deformations are in a high range as for PatientB.

4. Conclusions

In conclusion, the generalization of the *ZeroPressure* algorithm to be used on patient-specific geometries has been achieved through appropriate changes. Moreover, according to the parameters used in the analysis, the two configurations (with and without the pre-stress state) showed different outcomes in their TAVI simulations. This suggests that the inclusion of the pre-stress is important when simulating TAVI.

Future developments

The version of the *ZeroPressure* algorithm proposed in this work can be extended to complex models of either other sections of the aorta (aneurysm tracts, for example) or other vessels, for which the zero-pressure configuration needs to be obtained.

Regarding the TAVI simulations, a useful development would be to include the fluid field (FSI simulations), to better evaluate complications such as the paravalvular regurgitation (PLV) which cannot be studied with only structural analysis.

References

[1] C. Franceschelli and B. Fantaci, "Implementazione di un algoritmo elastostatico inverso con linearizzazione esatta per determinare la geometria vascolare scarica," 2021.

[2] A. N. Azadani *et al.*, "Comparison of mechanical properties of human ascending aorta and aortic sinuses," *Annals of Thoracic Surgery*, vol. 93, no. 1, pp. 87–94, Jan. 2012, doi: 10.1016/j.athoracsur.2011.08.002.

[3] G. Marom, "Numerical Methods for Fluid–Structure Interaction Models of Aortic Valves," *Archives of Computational Methods in Engineering*, vol. 22, no. 4, pp. 595–620, Nov. 2015, doi: 10.1007/s11831-014-9133-9.

[4] G. Luraghi *et al.*, "On the Modeling of Patient-Specific Transcatheter Aortic Valve Replacement: A Fluid–Structure Interaction Approach," *Cardiovasc Eng Technol*, vol. 10, no. 3, pp. 437–455, Sep. 2019, doi: 10.1007/s13239-019-00427-0.

[5] G. M. Bosi *et al.*, "A validated computational framework to predict outcomes in TAVI," *Sci Rep*, vol. 10, no. 1, Dec. 2020, doi: 10.1038/s41598-020-66899-6.